Developmental Cell *10*, 473–482, April, 2006 ©2006 Elsevier Inc. DOI 10.1016/j.devcel.2006.02.008

Hormonal Control of *C. elegans* Dauer Formation and Life Span by a Rieske-like Oxygenase

Veerle Rottiers,[1] Daniel L. Motola,[2] Birgit Gerisch,[3] Carolyn L. Cummins,[2] Kiyoji Nishiwaki,[4] David J. Mangelsdorf,[2] and Adam Antebi[1,*]
[1] Huffington Center on Aging
Department of Molecular and Cellular Biology
Baylor College of Medicine
Room M320
One Baylor Plaza
Houston, Texas 77030
[2] Howard Hughes Medical Institute
Department of Pharmacology
UTSW Medical Center
Room ND9.124A
6001 Forest Park
Dallas, Texas 75390
[3] Max Planck Institute for Molecular Genetics
Ihnestrasse 73
14195 Berlin
Germany
[4] RIKEN Center for Developmental Biology
Chuo-ku
Kobe 650-0047
Japan

Summary

***C. elegans* diapause, gonadal outgrowth, and life span are regulated by a lipophilic hormone, which serves as a ligand to the nuclear hormone receptor DAF-12. A key step in hormone production is catalyzed by the CYP450 DAF-9, but the extent of the biosynthetic pathway is unknown. Here, we identify a conserved Rieske-like oxygenase, DAF-36, as a component in hormone metabolism. Mutants display larval developmental and adult aging phenotypes, as well as patterns of epistasis similar to that of *daf-9*. Larval phenotypes are potently reversed by crude lipid extracts, 7-dehydrocholesterol, and a recently identified DAF-12 sterol ligand, suggesting that DAF-36 works early in the hormone biosynthetic pathway. DAF-36 is expressed primarily within the intestine, a major organ of metabolic and endocrine control, distinct from DAF-9. These results imply that *C. elegans* hormone production has multiple steps and is distributed, and that it may provide one way that tissues register their current physiological state during organismal commitments.**

Introduction

Nearly all species monitor their environment and physiology to regulate growth, metabolism, homeostasis, and reproduction. Metazoans employ neural and hormonal mechanisms to coordinate such processes throughout the body. During larval development, the nematode *C. elegans* assesses temperature, population density, food, and cholesterol availability to regulate alternative life history strategies. When favorable conditions prevail, animals develop rapidly from egg through four larval stages (L1–L4) to adult, a process termed reproductive growth. In unfavorable conditions, they arrest development at an alternative third larval stage, the dauer diapause, which is sexually immature, nonfeeding, stress resistant, and long lived (Riddle and Albert, 1997). Upon return to favorable conditions, dauer larvae will mature to normal adults. These life history alternatives have evolved to maximize reproductive success in the face of changing environments.

A molecular dissection of dauer diapause has led to key insights into conserved endocrine mechanisms regulating development, reproduction, and aging. Mutations in over 30 Daf (abnormal dauer formation) loci cause inappropriate dauer formation in response to the environment. Dauer-constitutive (Daf-c) mutants always form dauer larvae, while dauer-defective (Daf-d) mutants fail to enter diapause, irrespective of conditions. Cellular and molecular analyses reveal that environmental cues are detected by sensory neurons (Bargmann and Horvitz, 1991; Schackwitz et al., 1996), whose signals are transduced, in part, by cyclic guanosine monophosphate (cGMP) signaling (Birnby et al., 2000; Coburn et al., 1998; Komatsu et al., 1996) to regulate production of insulin/insulin growth factor I (IGF-I) and transformation growth factor-β (TGF-β) peptide hormones (Li et al., 2003; Murakami et al., 2001). Moreover, serotonergic and muscarinic neurotransmitters modulate these pathways (Sze et al., 2000; Tissenbaum et al., 2000). In favorable environments insulin/IGF-I and TGF-β pathways are active, promoting reproductive growth, while in unfavorable environments these peptide signaling pathways are suppressed, leading to diapause. While each pathway specifies some aspects of the dauer program independently—e.g., reduced insulin/IGF-I signaling principally promotes programs of stress resistance and longevity—they ultimately converge to mediate final commitments to dauer.

Evidently, both the TGF-β and insulin/IGF-I signaling pathways regulate diapause cell nonautonomously, suggesting that secondary hormones ensure organismal-wide coordination (Apfeld and Kenyon, 1998; Inoue and Thomas, 2000). One such signal may be a lipophilic hormone that regulates nuclear hormone receptor DAF-12 (Antebi et al., 2000). The cytochrome P450 (CYP450) DAF-9, which acts downstream of peptide hormonal pathways and upstream of DAF-12, is proposed to produce the DAF-12 ligand in favorable environments (Gerisch et al., 2001; Jia et al., 2002). It is regulated by upstream environmental and genetic inputs, works cell nonautonomously, and shows phenotypic congruence with DAF-12 ligand binding domain (LBD) mutants (Gerisch and Antebi, 2004; Mak and Ruvkun, 2004). Ultimately, *daf-12* dictates the choice between third stage reproductive growth versus diapause, and it is epistatic to most Daf loci for dauer formation (Riddle and Albert, 1997).

Several lines of evidence indicate that the DAF-12 ligand is a steroid. First, *daf-12* is homologous to vertebrate vitamin D, pregnane-X, and LXR receptors, which

*Correspondence: aantebi@bcm.tmc.edu

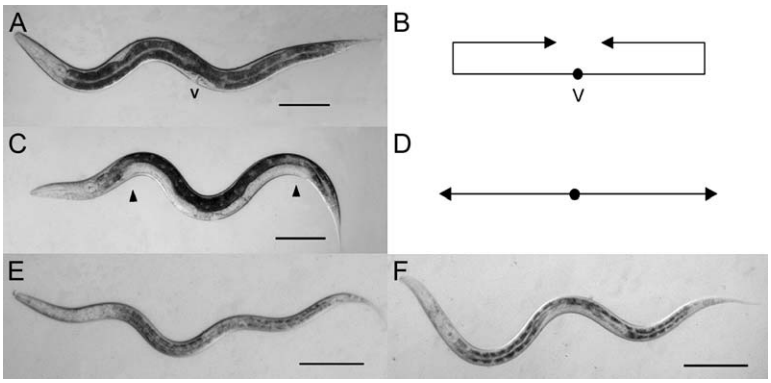

Figure 1. *daf-36* Mig Phenotype and Daf-c Phenotypes

(A) Wild-type L4 larva. The gonad (obscured here by the intestine) packs into the body cavity as two U-shaped arms. v, vulva.
(B) Schematic of wild-type gonadal outgrowth.
(C) *daf-36(dh303)* L4 larva on NG minus cholesterol. The gonadal Mig phenotype is seen as a ventral patch of white tissue (arrowheads) that extends into the head and tail.
(D) Schematic of *daf-36* gonadal outgrowth.
(E) Wild-type dauer larva.
(F) *daf-36(k114)* L3 partial dauer larva grown at 27ºC.
The scale bars are 100 μm; the left lateral aspect is shown.

use sterol metabolites as ligands, while *daf-9* is most homologous to CYP2 enzymes modifying sterols, fatty acids, and xenobiotics. Second, cholesterol deprivation mimics the phenotypes of *daf-9* and *daf-12* LBD mutants and enhances the phenotypes of hypomorphic mutants (Gerisch et al., 2001). Third, the Niemann Pick C1 homologs, which function in cholesterol trafficking (Ioannou, 2001), also work within the dauer pathway, proximal to *daf-9* and *daf-12*; *ncr-1 ncr-2* double mutants constitutively form transient dauer larvae (Li et al., 2004; Sym et al., 2000). Fourth, supplementation with crude lipid extracts rescues the Daf-c phenotypes of most mutants in the pathway, as well as dauers induced by culturing worms in the presence of the steroid lophenol and the absence of dietary cholesterol (Gill et al., 2004; Matyash et al., 2004). Consistent with the sterol hypothesis, recent work from our groups indicates that 3-keto sterols containing a (25S),26-carboxylic acid side chain behave as potent DAF-12 ligands and provide definitive evidence for the sterol hypothesis (Motola et al., 2006).

Hormones such as steroids, vitamin D, and bile acids are built sequentially by a series of enzymes that modify the original cholesterol backbone. A reasonable prediction of the hormone hypothesis is that the DAF-12 ligand is built in multiple steps. We therefore sought to find more genes in this putative hormone biosynthetic pathway. Here, we report the identification and analysis of a gene, *daf-36*, that encodes a Rieske-like oxygenase involved in the production of a DAF-12 ligand. To our knowledge, these studies are the first to ascribe this class of proteins to metazoan hormone metabolism.

Results

daf-36 Mutants Resemble *daf-9*

To find additional genes in hormone metabolism, we searched for other loci resembling *daf-9*. *daf-9* null mutants arrest as partially remodeled dauer larvae (partial dauers) at all temperatures and with complete penetrance, whereas hypomorphic *daf-9* mutants show a gonadal cell migration defect (Mig) during the L3 stage (Figures 1A–1D) (Gerisch et al., 2001). Both phenotypes are signatures of the lipophilic hormone branch of the dauer pathways.

Genetic screens for gonadal Mig mutants yielded alleles *k114* and *k122*, defining a locus on Chr. V dubbed *daf-36.* Like *daf-9* mutants, *daf-36* animals displayed gonadal Mig and Daf-c phenotypes, albeit weaker. Notably, upon outcrossing, Mig phenotypes became impenetrant (<2%), while partial dauer Daf-c phenotypes were apparent at 27ºC (Figure 1; Table 1). Unlike *daf-9*, the Daf-c phenotype was maternally rescued: homozygous offspring of heterozygous *daf-36*/+ mothers did not form dauers constitutively (Table 1). Noncomplementation screens yielded two additional alleles, *dh303* and *dh304*, the former giving somewhat more penetrant phenotypes at 27ºC (Table 1), but no significant change in the phenotypic spectrum.

daf-36 also demonstrated cholesterol-sensitive phenotypes, another signature of the lipophilic hormone pathway. We found that *daf-36* mutants cultured on NG plates without cholesterol displayed enhanced Mig phenotypes (Figure 1C; Table 1), similar to *daf-9* hypomorphs and *daf-12* LBD mutants (Gerisch et al., 2001). Moreover, *daf-36* genetically interacted with a *C. elegans* homolog of Niemann Pick C1, implicated in intracellular cholesterol transport. Interestingly, *daf-36 ncr-1* double mutants (but not *daf-36 ncr-2* double mutants) elicited a strongly synergistic Mig phenotype in the F1 generation (100% gonadal arms unreflexed; Table 1). These animals displayed other gonadal defects, including loose germ cells and protruding vulva, resulting in very small broods (8 ± 17, n = 30), significantly lower than *k114* itself (208 ± 23, n = 10). These findings are consistent with the notion that *daf-36* acts proximal to *ncr-1*, at a cholesterol-sensitive step.

Genetic Interactions

To pinpoint the position of *daf-36* within the dauer pathways, we performed genetic tests of epistasis and synergy. *k114* was used to construct doubles with null alleles of *daf-3* (SMAD) and *daf-5* (SNO/SKI), *daf-16* (FOXO), and *daf-12* (NHR), representing the transcriptional output of TGF-β, insulin/IGF-I, and nuclear receptor signaling, respectively. The resultant strains were analyzed for Daf-c phenotypes at 27ºC (Table 1). At this temperature, *daf-36* formed about 42% dauer larvae. *daf-12* efficiently suppressed this phenotype, while *daf-3* and *daf-5* did not (Table 1). Since *daf-3* alone formed 34% dauers at 27ºC, consistent with previously reported data (Ailion and Thomas, 2003), we also scored dauer formation at 25ºC, a temperature at which *daf-3* is dauer defective. We found that 48% of *daf-36 daf-3* animals formed dauers, showing that *daf-36* enhances the Daf-c phenotype of *daf-3* at a temperature at which it is usually Daf-d. Doubles with *daf-16* formed 21%

Table 1. Phenotypes of *daf-36* and Double Mutants

Strain	Daf-c at 25ºC ± SE[a] (%)	N[b]	Daf-c at 27ºC ± SE[a] (%)	N[b]	Mig at 20ºC NG-chol[c] (%)
N2	0 ± 0	777 (3)	0 ± 1	3774 (8)	0
daf-36(k114)	2 ± 1	845 (2)	42 ± 18	3600 (8)	35
k122	1 ± 2	798 (2)	38 ± 17	2287 (6)	26
dh303	7 ± 2	602 (2)	61 ± 21	1949 (5)	55
dh304	4 ± 1	695 (2)	61 ± 27	1815 (5)	42
F1 progeny of N2 males × *k114*	nd		0[d]	> 200	nd
Progeny of *k114*/+	nd		0[e]	> 200	nd
F1 progeny of *sDf35*/+ and +/+ males × *k114*	nd		9[f] ± 0	816 (2)	nd
daf-36(k114)dhEx320(daf-36::gfp)	nd		0 ± 0	400 (2)	nd
daf-3(mgDf90)	0 ± 0	684 (2)	22 ± 18	1587 (4)	nd
daf-36(k114);daf-3(mgDf90)	48 ± 23	531 (2)	98 ± 29	906 (3)	nd
daf-5(e1386)	0 ± 0	593 (2)	0 ± 0	1377 (3)	nd
daf-36(k114);daf-5(e1386)	1 ± 0	705 (2)	33 ± 14	1333 (3)	nd
daf-16(mgDf50)	0 ± 0	620 (2)	0 ± 0	1389 (4)	nd
daf-36(k114);daf-16(mgDf50)	3 ± 4	515 (2)	21 ± 7	1862 (4)	nd
daf-12(rh61rh411)	0 ± 0	726 (3)	0 ± 0	924 (3)	nd
daf-36(k114);daf-12(rh61rh411)	0 ± 0	669 (3)	0 ± 0	936 (3)	nd
daf-9(k182)	1 ± 1	448 (2)	41 ± 2	808 (2)	nd
daf-36(k114);daf-9(k182)[g]	100 ± 0	281 (4)	nd	nd	nd
daf-36(k114);dpy-7::daf-9::gfp +	nd		0 ± 0	336 (2)	25
daf-36(k114);dpy-7::daf-9::gfp −	nd		32 ± 14	286 (2)	13
ncr-1(nr2022)	0 ± 0	502 (2)	17 ± 23	599 (2)	0
ncr-2(nr2023)	0 ± 0	671 (2)	0 ± 0	465 (2)	0
ncr-1(nr2022)ncr-2(2023)	66 ± 15	682 (2)	73	329	nd
ncr-1;daf-36(k114)	nd		nd	nd	100[h]
ncr-2;daf-36(k114)	0 ± 0	435 (2)	59 ± 55	449 (2)	nd

nd, not determined.
[a] Dauers formed under reproductive growth conditions.
[b] Number of experiments is given in parentheses.
[c] Hermaphrodite distal tip cells that fail to turn in L3, n > 50 cells, grown on NGM without added cholesterol.
[d] Percent Daf-c F1 progeny from cross of wild-type males × *k114* hermaphrodites.
[e] Percent Daf-c F1 progeny from mothers heterozygous for *daf-36*.
[f] Deletion *sDf35* was tested in strain BC2511. Heterozygous hermaphrodites were crossed to wild-type males. The resulting males were then crossed to *k114* hermaphrodites. 25% of the progeny are expected to be *k114*/*sDf35*. Since *k114* controls form 42% dauers, 10% dauers are expected if *k114* falls into *sDf35*.
[g] Measured from *k114 k182* homozygotes that have lost the *daf-36*(+); *sur-5::gfp* extrachromosomal array *dhEx315*. This strain is unconditionally Daf-c: similar results are obtained at 15ºC and 20ºC.
[h] *ncr-1 k114*, hermaphrodite distal tip cells that fail to turn in L3, n > 50 cells, cultured on normal NGM plates containing 5 μg/ml cholesterol.

partial dauers at 27ºC, and a low percentage of partial dauers were also found at 25ºC, possibly showing a weak *daf-16* dependence. Thus, *daf-36* largely acts downstream or parallel to TGF-β and insulin/IGF-I signaling, but upstream of DAF-12. This pattern of epistasis resembles *daf-9*, lending further support to the idea that *daf-9* and *daf-36* work at a similar point in the dauer circuits.

Accordingly, we found that *daf-36(k114)* synergistically interacted with *k182*, a weak allele of *daf-9*, to form Daf-c dauer larvae nonconditionally with complete penetrance, similar to *daf-9* nulls (Table 1). Moreover, *daf-9 daf-36* double null mutants were indistinguishable from *daf-9* mutants alone (data not shown), suggesting that they ultimately influence the same process. Finally, overexpression of *daf-9* in the hypodermis (a syncitial epidermal tissue surrounding the worm), under the control of the *dpy-7* promoter (*dhEx217*), fully suppressed *daf-36* Daf-c phenotypes, but not gonadal Mig phenotypes (Table 1). These results suggest that *daf-9* is rate limiting for diapause regulation.

Life Span Phenotypes

It was shown (Hsin and Kenyon, 1999) that ablation of the germline lengthens the life span of wild-type animals by 60%, an effect offset by additional ablation of the somatic gonad, suggesting that germline and somatic gonad produce antagonistic signals regulating longevity. The longevity of germline-ablated animals is abrogated in *daf-16*, *daf-12* (Hsin and Kenyon, 1999), and *daf-9* mutants (Gerisch et al., 2001), revealing that components of insulin/IGF-I and sterol hormone signaling are required to promote long life. Similarly, we found that *daf-36* germline-ablated animals did not live longer than untreated controls (Figure 2), showing that longevity associated with germline ablation also requires *daf-36(+)*. As with *daf-9*, the ablation of the somatic gonad did not shorten life span any more than germline ablations.

Previous studies had also shown that strong *daf-9* mutants recovered to adult live about 25% longer than wild-type at 15ºC (Gerisch et al., 2001; Jia et al., 2002), while hypomorphic *daf-9* mutants did not. In this context, *daf-36(k114)* mutants behaved like *daf-9* hypomorphs, with little influence on life span (data not shown).

daf-36 Encodes a Rieske-like Oxygenase

daf-36 was mapped to chromosome V between *unc-42* and *sma-1*, and within deletions *sDf35* and *mDf1*. Fine mapping with snipSNPs and sequencing SNPs (Wicks

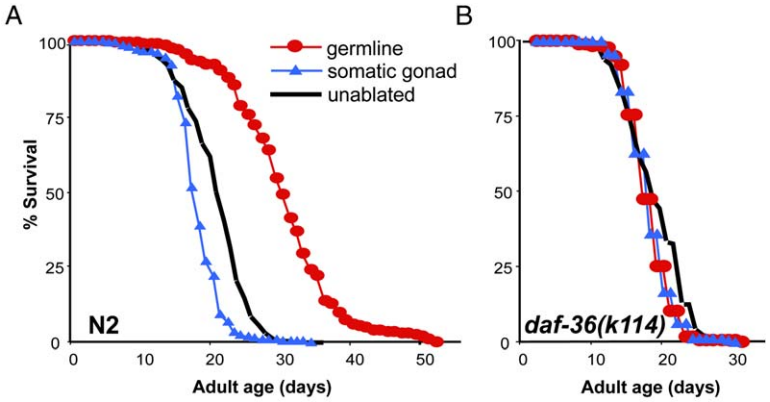

Figure 2. Effect of Germline and Gonad Ablation on *daf-36(k114)* at 20ºC

(A and B) Life span of (A) wild-type and (B) *daf-36(k114).*

(C) Mean and maximum life span. Significance tests are against N2 control unless indicated. *Significant in t test ($p<0.0001$). [1]Number of experiments in parentheses. [2]Tested against *k114* control.

C

Strain	Treatment	Mean ± SE [days]	Maximum ±SE [days]	N[1]
N2	unablated	21.7 ± 1.4	30.7 ± 3.5	720(6)
	germline	31.7 ± 1.7*	50.7 ± 3.4	251(6)
	somatic gonad	18.7 ± 1.3*	29.8 ± 3.7	381(6)
daf-36(k114)	unablated	19.8 ± 0.8*	29.0 ± 1.0	300(3)
	germline	18.0 ± 1.1[2]	28.0 ± 3.1	188(2)
	somatic gonad	18.1 ± 1.0[2]	29.5 ± 1.0	143(2)

et al., 2001) delimited the region to three cosmids, one of which (F21F2) rescued the Daf-c and Mig phenotype of *daf-36(k114)* (Figure 3A). The sequence of genes in the region revealed mutations in C12D8.5, which was further confirmed by transgenic rescue. The C12D8.5 coding region was determined by sequencing cDNAs yk722g3, yk744h10, and yk743b11, which correspond to a single transcript encoding a protein of 428 amino acids (Figure 3B).

Homology searches revealed that DAF-36 is related to Rieske-like oxygenases of plants and bacteria: proteins that contain a Rieske-like FeS coordination center (Iwata et al., 1996), presumably involved in redox reactions, and a nonheme iron binding domain, involved in oxygen binding and catalysis (Figure 3C). The known bacterial homologs typically catalyze the *cis* oxygenation of aromatic structures (Jiang et al., 1996). Interestingly, *Rhodococcus erythropolis kshA*, *daf-36*'s closest bacterial

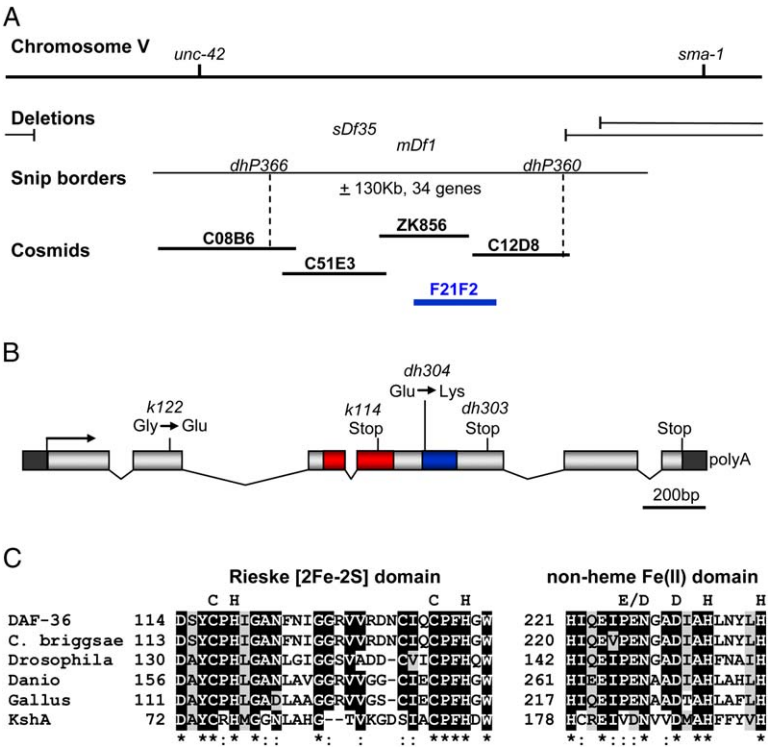

Figure 3. Structure of the *daf-36* Locus, Gene, and Protein Domains

(A) Genetic and physical map; the blue cosmid F21F2 rescues *daf-36(k114)* mutant phenotypes.

(B) Structure of the *daf-36* gene with position of mutations. Black arrow, initiator methionine; gray box, exons; black box, 5′ and 3′ UTRs; polyA, polyadenylation site; red box, Rieske iron sulfur domain; blue box, nonheme iron domain.

(C) Alignment of the Rieske domain and the nonheme iron binding domain of DAF-36 and close homologs. Consensus sites are marked above sequence. Positions at which 80% identity is found are marked black. AA with the same properties are marked in gray. Positions with 100% similarity are marked with an asterisk. Positions with high similarity are marked with a colon. DAF-36 is C12D8.5 wormbase protein CE34156, *C. briggsae* is *Caenorhabditis briggsae* protein CBG095563, *Drosophila* is *Drosophila melanogaster* protein CG40050 (NP_10153), *Danio* is *Danio rerio* predicted protein zgc:92275, *Gallus* is *Gallus gallus* predicted protein XP_425346.1, and *kshA* is *Rhodococcus erythropolis* protein AAL96829 (van der Geize et al., 2002).

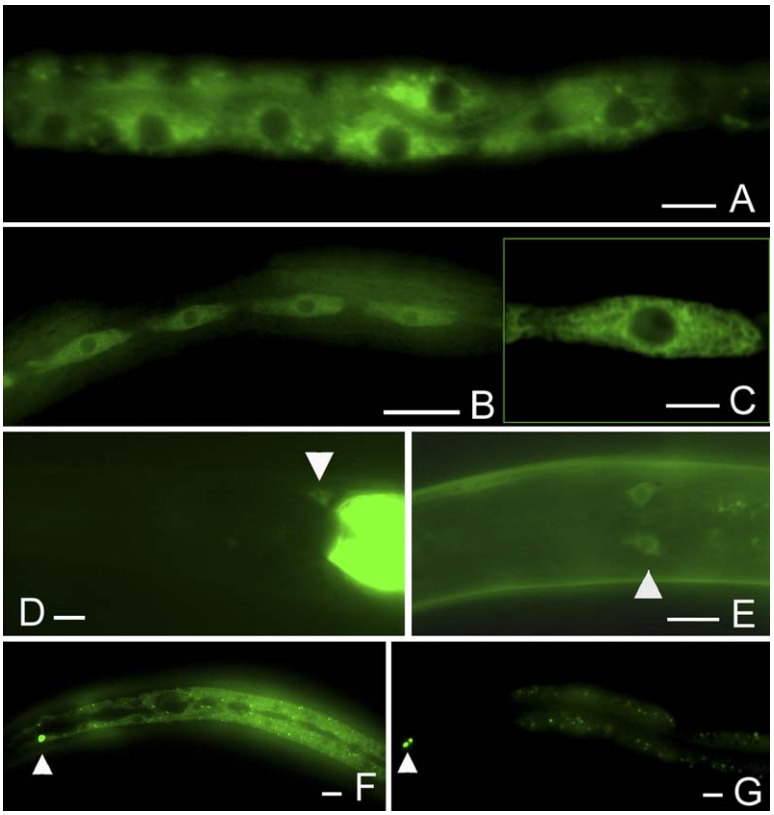

Figure 4. *daf-36::gfp* Expression Pattern and Evidence for Hormonal Feedback

(A–E) *daf-36::gfp* expression. (A) Intestine of a wild-type L1 larva. (B) Seam cells of a *daf-2(e1370)* L2d larva. (C) Detail of seam cell. (D) Head mesodermal cell of an adult worm. (E) Head of L2d larva; the arrowhead points to neurons.

(F–G) *daf-9::gfp* expression at 20°C. Arrows point to the XXX cells, which do not change expression. (F) *daf-36(k114)* L3 larva with strong hypodermal expression. (G) N2 L3 larva, with low hypodermal expression.

(A)–(D), (F), and (G) show the left lateral aspect; (E) shows the ventral aspect. The scale bars in (A) and (C)–(G) are 10 μm; the scale bar in (B) is 50 μm.

relative of known function, is implicated in the metabolism of steroids (van der Geize et al., 2002), catalyzing the 9-α hydroxylation of 4-androstene-3,17-dione and 1,4-androstadiene-3,17-dione (van der Geize et al., 2002). This chemistry suggests that *daf-36* could also modify a sterol derivative.

Two other proteins are found in *C. elegans* that contain a Rieske domain, but both lack the nonheme iron binding domain. *isp-1* is a mitochondrial protein whose mutant phenotypes include slow growth and long life (Feng et al., 2001), while F20D6.11 is unstudied. A phylogenetic analysis revealed that *daf-36*, *isp-1*, and F20D6.11 map onto the three broad classes of the Rieske proteins, the Rieske-like oxygenases, and the Rieske ferredoxins, respectively (Schmidt and Shaw, 2001) (Figure S1; see the Supplemental Data available with this article online).

Among metazoans, clear orthologs are found in other nematodes, insects, amphibians, fish, and birds, including model genetic organisms such as Zebrafish and *Drosophila*, with overall identities ranging from 35% to 45% (Figure 3C; Figure S2). Surprisingly, no clear mammalian orthologs were detected. Multiple sequence alignment of the orthologs revealed two additional homology domains near the N and C termini (Figure S2). The C-terminal domain includes a conserved aspartate residue implicated in coordination of Fe. As these proteins have no defined physiological role, the studies here imply that *daf-36* and relatives function in metazoan hormone metabolism.

Molecular Lesions

The sequence of *daf-36* alleles revealed that they disrupt key regions of the protein. *k114* and *dh303* were both nonsense mutations resulting in premature stops (Figure 3B; Figure S2). The earliest stop, *k114*, is a candidate null because it lacks the nonheme iron binding domain necessary for oxygenase function (Jiang et al., 1996). Accordingly, placing *daf-36(k114)* over a deletion did not enhance the phenotype (Table 1). *dh303* truncated the protein upstream of the C-terminal homology region, but it produced mutant phenotypes at least as severe as *k114* (Table 1). *k122* was a missense mutation in a conserved glycine residue that affected the N-terminal homology region, while *dh304* was a missense mutation in a nonconserved residue proximal to the nonheme iron binding domain.

Expression Pattern

To analyze the *daf-36* expression pattern, we constructed a gene fusion containing 1.3 kb of promoter and the 2.2 kb *daf-36* genomic coding region fused at its C terminus to *gfp*. This fusion was functional, as measured by rescue of Daf-c phenotypes, reducing dauer formation to 0% at 27°C (Table 1). *daf-36::gfp* was most strikingly expressed in the intestinal cytoplasm (Figure 4A) at all postembryonic stages, including dauer. In addition, *daf-36::gfp* was seen in the head mesodermal cell (Figure 4D), a cell whose function is unknown but which makes gap junctions with adjacent body muscles (White et al., 1976). Occasionally, very faint expression was seen within two unidentified head neurons (Figure 4E), posterior to the nerve ring, which were clearly distinct from the XXXR/L, the neuroendocrine cells that express DAF-9 and NCR-1,2 proteins (Li et al., 2004; Ohkura et al., 2003). During the L2d stage, prior to entry into dauer diapause, neuronal expression

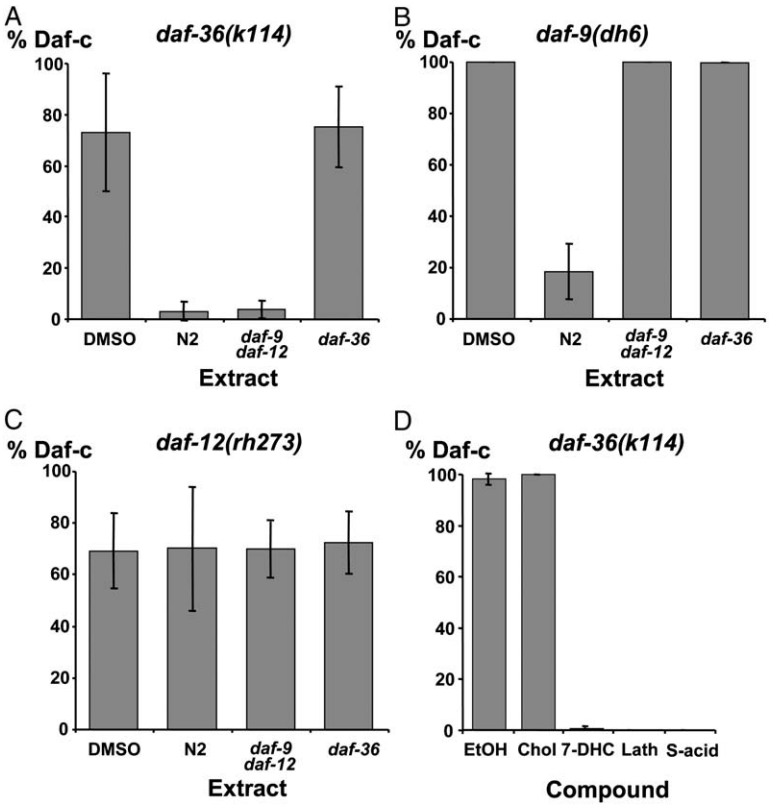

Figure 5. Rescue of Daf-c Phenotypes by Lipid Extracts and Nematode Steroids

(A–D) Rescue of Daf-c phenotypes by (A–C) lipid extracts and (D) compounds. (A) *daf-36(k114)* rescue by lipid extracts. (B) *daf-9(dh6)* rescue by lipid extracts. (C) *daf-12(rh273)* is not rescued by lipid extracts. (D) *daf-36(k114)* rescue by steroid compounds. EtOH is the ethanol control, Chol is 33.3 μM cholesterol, 7-DHC is 33.3 μM 7-dehydrocholesterol, Latho is 33.3 μM lathosterol, and S-acid is 250 nM Δ^4-dafachronic acid. Error bars represent the standard deviation derived from at least two independent experiments.

increased slightly, and, surprisingly, expression commenced in the seam cells (Figures 4B and 4C), epidermal cells located at the lateral midline. Visible also in *daf-2*, *daf-7*, and *daf-11* Daf-c dauers as well as in normal dauers, epidermal *daf-36::gfp* appeared to be localized in a cytosolic meshwork. Given that the primary role of *daf-36(+)* is to avert diapause, epidermal expression in L2d larvae could poise the animal for efficient dauer exit.

We observed that overall *daf-36::gfp* expression was visibly reduced in *daf-2(e1370)* background (25ºC, data not shown), but we saw no obvious changes in *daf-7*, *daf-11*, *daf-9*, *daf-12*, *daf-16*, *daf-5*, and *daf-3* mutants. In addition, *daf-36* mutants influenced the expression of *daf-9::gfp*, causing an upregulation in the hypodermis during mid-larval development (Figures 4F and 4G). Such upregulation is also seen in *daf-9* hypomorphs, and it is posited to reflect homeostatic feedback that maintains reproductive hormone levels within normal bounds (Gerisch and Antebi, 2004). Such regulation further solidifies the role of *daf-36* in the hormone pathway and suggests that *daf-36* works upstream of *daf-9*.

Rescue of *daf-36* Mutant Defects by Lipid Extracts

Recent studies have found that lipid extracts from synchronized L3 larvae rescue the Daf-c phenotypes of *daf-9*/CYP450 mutants, but not those of *daf-12* LBD mutants (Gill et al., 2004). If, as predicted, *daf-36* is involved in lipophilic hormone production, then lipid extracts from wild-type worms should also supplement the hormone deficiency in a DAF-12-dependent manner. Similarly, we prepared crude lipid extracts and found that they contained rescuing activity (Figure 5A). Whereas wild-type extracts fed to *daf-36* mutants potently reversed the Daf-c phenotypes at 27ºC, extracts from *daf-36* mutants did not, nor did additional cholesterol (Figures 5A and 5D). Similarly, wild-type extracts rescued the Daf-c phenotypes of *daf-9* mutants, while *daf-9 daf-12* extracts did not (the *daf-12* null permits growth of *daf-9* null mutants without dauer arrest) (Figure 5B). By contrast, wild-type extracts failed to substantially rescue the phenotypes of LBD mutants *daf-12(rh273)* (Figure 5C) and *daf-12(rh61)* (data not shown), which are predicted to be ligand insensitive.

We further reasoned that extracts derived from different biosynthetic mutants could be used to order their functions in a pathway. In principle, upstream mutants fed extracts derived from downstream mutants should bypass the block, complete hormone synthesis, and overcome phenotypic defects. Conversely, downstream mutants fed extracts from upstream mutants would not be rescued. Interestingly, we found that extracts from *daf-9 daf-12* animals potently rescued the Daf-c defects of *daf-36*, whereas extracts from *daf-36* animals failed to rescue either *daf-36* or *daf-9* (Figures 5A and 5B). These results support the notion that *daf-36* works upstream or parallel to *daf-9*.

Rescue of *daf-36* Mutant Defects by Steroids

Recent work from our groups indicate that 3-keto sterols containing a (25S),26-carboxylic acid side chain, termed dafachronic acids, behave as potent DAF-12 ligands (Motola et al., 2006). If DAF-36 participates in the production of a DAF-12 hormone, then the chemically identified ligand should bypass mutant phenotypes. Indeed, we found that Δ^4-dafachronic acid potently rescued *daf-36* Daf-c phenotypes in the 100 nM

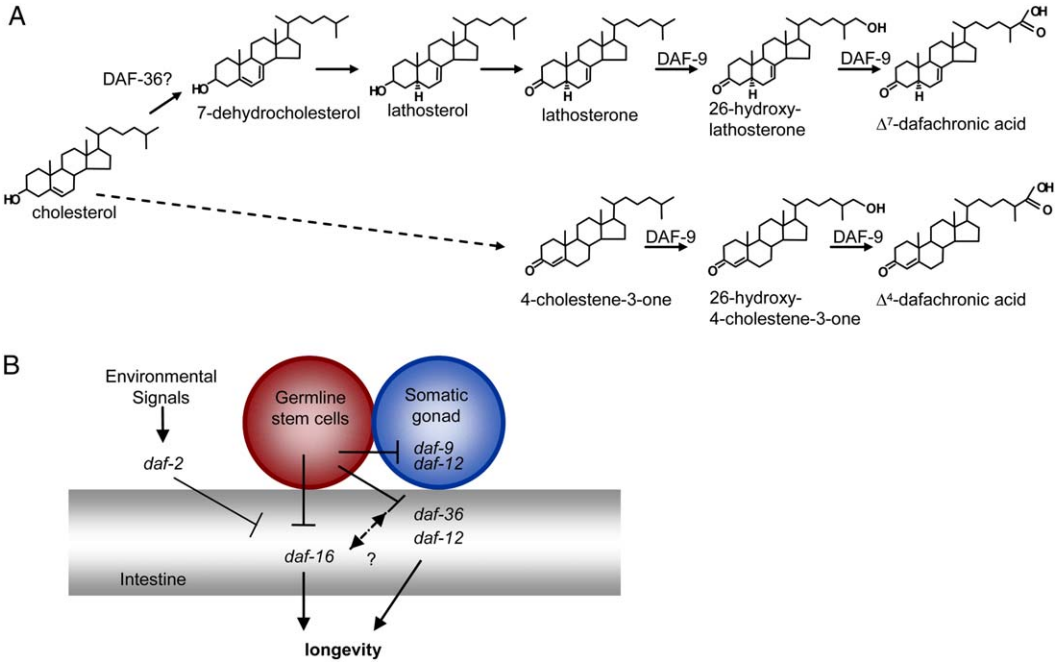

Figure 6. Models for *daf-36* Biochemical and Physiological Action

(A) Speculative model of the DAF-12 ligand biosynthetic pathway. This pathway is modified from the pathways by Chitwood (1999) and Motola et al. (2006).

(B) Model for regulation of life span by gonadal signals (see text).

range, comparable to what is seen with *daf-9* (Figure 5D). Rescue was diminished or absent in *daf-12* LBD mutants (data not shown).

If DAF-36 works upstream or parallel to DAF-9, then DAF-9 substrates should rescue *daf-36* mutants. We tested the DAF-9 substrates lathosterone and 4-cholestene-3-one and found that these compounds indeed rescued *daf-36* mutant phenotypes (Figure S3). We further tested cholesterol as well as 7-dehydrocholesterol and lathosterol, which are proposed to be the early metabolites of cholesterol (Chitwood, 1999; Motola et al., 2006) (Figures 5D and 6A; Figure S3). All compounds, except cholesterol, rescued the *daf-36* Daf-c phenotype, suggesting that *daf-36* may act at an early step of hormone metabolism, possibly converting cholesterol to 7-dehydrocholesterol (Figures 5D and 6A; Figure S3).

Discussion

DAF-36 Rieske-like Oxygenase Produces a DAF-12 Hormone

Our studies are among the first to ascribe a role for metazoan Rieske-like oxygenases in lipophilic hormone production. This hormone regulates *C. elegans* dauer diapause, gonadal outgrowth, and adult longevity in the germline pathway. Multiple lines of evidence argue that the *daf-36* Rieske-like oxygenase is involved in the production of a DAF-12 ligand. Importantly, the spectrum of *daf-36* phenotypes closely resembles those seen in mutants acting proximal to hormone production, transport, or binding. First, *daf-36* forms partial dauers, like *daf-9* mutants and *daf-12* ligand binding domain mutants (Gerisch et al., 2001; Jia et al., 2002). The formation of such partial dauers is primarily found in genes acting downstream of insulin/IGF-I, TGF-β, and cGMP signaling. Second, *daf-36* displays gonadal migration phenotypes, as seen in hypomorphic alleles of *daf-9* and *daf-12* ligand binding domain mutants. Third, *daf-36* mutants are sensitive to cholesterol deprivation, showing that *daf-36* acts at a cholesterol-sensitive step proximal to *daf-9* and *daf-12*. In support of this, *daf-36* interacts synergistically with *ncr-1*, one of the *C. elegans* homologs of human Niemann-Pick type C1 disease, which are implicated in cholesterol trafficking (Sym et al., 2000; Li et al., 2004; Ioannou, 2001). Fourth, genetic epistasis showed that *daf-36* acts at the same step in the pathway as *daf-9*, downstream of the transcriptional outputs of insulin/IGF-I and TGF-β signaling, but upstream of *daf-12*. Finally, like *daf-12* and *daf-9*, *daf-36* is required for the life span-enhancing signal of the gonad. These phenotypic similarities alone argue for a similar function between *daf-9* and *daf-36*.

Our view that *daf-36* is involved in the production of a DAF-12 ligand is bolstered by its molecular identity. *daf-36* encodes a protein that is homologous to the catalytic subunit of a Rieske-like ring hydroxylating oxygenase, consistent with modification of a lipophilic substrate. In particular, the homology of DAF-36 to *kshA*, a subunit of a ketosteroid hydroxylase of *Rhodococcus erythropolis* (van der Geize et al., 2002), is intriguing and suggests a possible function in sterol metabolism. Accordingly, the *Drosophila* ortholog, *Neverland*, has been recently implicated in early steps of ecdysteroid biosynthesis, and it is expressed in the prothoracic gland, a key endocrine tissue, suggesting a phyletically conserved role in hormone production (R. Niwa and H. Kataoka, personal communication). In *C. elegans*, expression of *daf-36* is limited to a few tissues—intestine,

neurons, HMC, and seam cells—that affect programs throughout the organism, also consistent with endocrine control. Finally, crude lipid extracts, a chemically defined DAF-12 ligand, Δ^4-dafachronic acid, the *daf-9* substrates, as well as the putative precursors to the *daf-9* substrates potently rescued *daf-36* Daf-c phenotypes. In sum, these results provide strong evidence that DAF-36 works in the production of a DAF-12 ligand.

daf-36/daf-9 Interaction

So far, our results suggest that *daf-36* could work upstream or parallel to *daf-9*. We observed that lipid extracts derived from *daf-9* mutants could rescue *daf-36* mutants, but not vice versa. The simplest interpretation of vectorial rescue is that *daf-36* works upstream of *daf-9* (with the caveat that *daf-9* rescue might be more stringent, or *daf-36* metabolic intermediates unstable). Accordingly, identified DAF-9 substrates, as well as upstream metabolites, rescued *daf-36*, implying that these compounds work downstream or bypass the *daf-36* block. By contrast, cholesterol and cholesterol derivatives (V.R., unpublished data) failed to rescue, suggesting an early role in the conversion of cholesterol. Similarly, the *Drosophila Neverland* is thought to work early on in the ecdysone biosynthetic pathway (R. Niwa and H. Kataoka, personal communication). In addition, the fact that *daf-36* influenced *daf-9* hypodermal feedback regulation may indicate an upstream role. Finally, the fact that DAF-9-generated reaction products serve directly as potent DAF-12 ligands suggests that DAF-9 works at a final step in hormone synthesis (Motola et al., 2006). By inference, DAF-36 must work upstream.

The *daf-36* null phenotype is substantially weaker than the *daf-9* mutant phenotype, which argues against a strict linear pathway and instead suggests parallel pathways. Accordingly, preliminary genetic screens looking for *daf-36* enhancers suggest that such parallel functions indeed exist (V.R. and A.A., unpublished data). In addition, DAF-9 has been found to use at least two different substrates in cell culture assays, lathosterone and 4-cholestene-3-one (Motola et al., 2006), to produce two ligands for DAF-12 of different potency. Conceivably, *daf-36* could be involved in the production of one of these substrates or yet another substrate. Since 7-dehydrocholesterol rescues both the *daf-36* and *Neverland* mutant phenotypes, a reasonable hypothesis is that they act in the conversion of cholesterol to 7-dehydrocholesterol (Figure 6A). In worms, the conversion of 7-dehydrocholesterol to lathosterol (Chitwood, 1999) could then lead to the production of lathosterone, a *daf-9* substrate. Finally, the *daf-9* metabolite of lathosterone, Δ^7-dafachronic acid, is a high-affinity ligand for DAF-12 (Figure 6A) (Motola et al., 2006). Although this model is still speculative, it provides a plausible outline for the hormone biosynthetic pathway.

The Rieske Proteins

daf-36 and its metazoan homologs cluster within the so-called Rieske-type oxygenases (Figure S1). This cluster likely reflects an ancient role in oxidizing ringed or aromatic structures. In contrast to CYP450, which use heme for iron binding, the nonheme iron binding domain of such oxygenases uses two histidines and one carboxylate moiety to chelate iron(II), leaving three open valences for the binding of ligand and molecular oxygen (Que, 2000). This creates a different steric geometry and allows for more versatile chemistry. In particular, such oxygenases are able to catalyze hydroxylation or epoxidation, like heme proteins, but can additionally catalyze oxidative cleavage of catechols, arene *cis*-hydroxylation, oxidative ring opening or closure, and desaturation (Que, 2000). Conceivably, DAF-36 could act as a desaturase or oxidize the cholesterol backbone.

DAF-36 homologs are broadly distributed throughout phylogeny, from bacteria, plants, invertebrate, and lower vertebrate species. Aside from the *C. elegans* and *D. melanogaster* genes, only the plant enzymes have been intensively studied in eukaryotes, and these function in chlorophyll metabolism and leaf senescence (Gray et al., 2004). Curiously, no mammalian orthologs of DAF-36 could be found. Possibly, such an enzyme is present but not easily recognized, since only three amino acids constitute the iron chelating residues of the nonheme iron binding domain (Que, 2000). Alternately, its role in hormone metabolism may have been subsumed by other oxygenases such as cytochrome P450s.

Germline Signaling and Hormonal Regulation of Life History

In *C. elegans*, signals from the germline influence adult life span (Hsin and Kenyon, 1999). The proliferating germline stem cells are found to be the source of a germline signal that shortens life (Arantes-Oliveira et al., 2002). When this signal is absent, animals live longer, and this extension depends on functional *daf-12*, *daf-16* (Hsin and Kenyon, 1999), and *daf-9* (Gerisch et al., 2001). *daf-16* is required specifically during adulthood (Arantes-Oliveira et al., 2002) and in the intestine for germline signaling (Libina et al., 2003). The dependence on *daf-9* and *daf-12* has not been specified further. Gonadal cells possibly influence the production of, or the response to, a steroid hormone that promotes longevity (Arantes-Oliveira et al., 2002). A simple hypothesis is that this hormone is produced by DAF-9 and binds to DAF-12.

We now show that germline ablation in *daf-36* also abrogates life span extension, suggesting that *daf-36* is necessary for germline signaling. On their own, *daf-36* mutants display relatively normal development, fertility, and life span, and phenotypes in dauer formation and gonad migration are relatively mild. Nevertheless, suppression of germline longevity is robust. If *daf-36* has a direct role in this pathway, it, like *daf-9*, probably acts downstream or parallel to the germline signal. In a simple model, germline stem cells in reproductive mode could normally both prevent nuclear localization of DAF-16 in the intestine and (as a result of this or independently) modify a hormonal signal through *daf-9*, *daf-36*, and *daf-12* (Figure 6B). Consequently, longevity genes are silenced. When germline signals are removed, longevity genes are activated by DAF-16 and by the resultant hormonal signal of DAF-36/DAF-9/DAF-12. Presently, it is unknown whether *daf-16* works independently of *daf-36*/*daf-9*/*daf-12* in this context.

Metazoan endocrine signaling often entails a complex interplay between various tissues, which collectively determine the overall outcome of organismal commitments. For *C. elegans* life span regulation, the intestine

is primary, and the nervous system and other tissues are secondary, for *daf-16*-mediated longevity (Libina et al., 2003). These tissues control life span and diapause cell nonautonomously, in part through regulation of insulin signals themselves as well as other presumed hormones (Murphy et al., 2003). It is intriguing that *daf-36* is also expressed in the intestine and influences longevity in the germline pathway. However, germline ablation does not overtly regulate *daf-36* expression (V.R. and A.A., unpublished data).

For diapause or life span regulation, the nonoverlapping expression patterns of *daf-36* and *daf-9* reveal that sites of hormone production are distributed. Moreover, the influence of *daf-36* on *daf-9* expression also reveals a complex interplay of the pathway between these tissues through feedback. DAF-36 expression in the intestine places it within a major organ of dietary cholesterol uptake, lipid metabolism, and endocrine regulation, speculatively providing one of the earliest signals in the hormone pathway. Distributed synthesis may permit local production of specific active hormones in peripheral tissues. In addition, it may provide one mechanism by which tissues can cast their vote during organismal decision making, or register their current physiological state. In particular, the intestine is well poised to assess dietary input, which can then be conveyed to other tissues, thus coordinating organismal metabolism, life history strategies, reproduction, and life span.

Experimental Procedures

Culture Conditions and Mutant Isolation

Nematode stocks were cultured at 20ºC on NG agar seeded with *E. coli* strain OP50 unless indicated otherwise. NG contains cholesterol added to 5 μg/ml. NG minus cholesterol medium omits cholesterol. *k114* and *k122* were isolated in F2 screens for animals with displaced gonadal tissue on ventral or dorsal surfaces, after 0.5% ethylmethanesulfonate (EMS) mutagenesis. For the noncomplementation screens, EMS-mutagenized N2 males were mated to *daf-36(k114) dpy-11(e224)* hermaphrodites on NG minus cholesterol plates. A total of 15,000 genomes were examined for F1 transheterozygotes with the Mig phenotype to obtain *dh303* and *dh304*. Mutants were outcrossed at least three times.

Positional Cloning of *daf-36*

Three-factor mapping was done as described in Sulston and Hodgkin (1988). For snipSNP mapping, we used the triple mutant *unc-42(e270) daf-36(k114) sma-1(e30)* obtained from the three-factor mapping. The triple mutant was crossed to the wild-type strain CB4856. Recombinants were picked, and SNPs were analyzed as described in Wicks et al. (2001). Cosmids were microinjected (10–20 ng/μl) into *daf-36(k114)* and *daf-36(k122)* along with the pTG96 *sur-5::gfp* (Yochem et al., 1998) transformation marker (75–100 ng/μl). All seven F21F2 lines rescued the *k114* Daf-c phenotype at 27ºC and the Mig phenotype on NG minus cholesterol plates.

Molecular Biology

For *daf-36::gfp* construction, a 3.5 kb genomic fragment containing the *daf-36* coding region and 1.3 kb upstream was amplified with primers 5′-CGACCGGTGAGTCAAAAATTGATTTTGC-3′ (forward) and 5′-CGACCGGTGAGTCAAAAATTGATTTTGC-3′ (reverse) and cloned into pCR-Blunt II-TOPO vector (Invitrogen). AgeI/PstI/DraIII-digested *daf-36*-TOPO was then inserted into AgeI/PstI-digested *gfp* vector L3781 (Fire vector kit 1997). The construct was injected (*daf-36::gfp* [10 ng/μl]) both with the *lin-15(+)* marker (75 ng/μl) into *lin-15(n765)* animals and without marker in N2 worms. *dhEx317* and *dhEx320 (lin-15(+))* and *dh321* and *dh322* (no marker) extrachromosomal lines fully rescued *daf-36(k114)* Mig and Daf-c phenotypes.

Life Span Assays

Adult life span assays and gonadal cell ablation experiments were performed as described (Gerisch et al., 2001). Day 0 corresponds to the L4 stage. Life span of gonad and germline-ablated *daf-36(k114)* was determined in two independent experiments at 20ºC. As many as one-third of Z2–Z3-ablated animals for *k114* and N2 exploded as adults and were excluded from analysis. Statistical analyses were performed with the Excel 98 Student's t test.

Lipid Extracts

N2, *daf-12(rh61rh411); daf-9(dh6)*, *daf-36(k114)*, and *daf-36(k114) daf-12(rh61rh411)* worms were grown in bulk on 21 cm square dishes (Nunc). Adults were harvested and bleach treated. The eggs were transferred to liquid culture (S-complete medium supplemented with OP50) and grown at 22.5ºC. After 2 days, synchronized cultures of L3–L4s were harvested, flash frozen in liquid nitrogen, and stored at −80ºC. Extracts were made fresh before each test from about 2 g worms/extract. The sonicated worms were ether extracted, and the resulting lipids were weighed and diluted in DMSO. Typically, about 20 mg lipids were obtained and diluted in DMSO (X mg extract in 3X μl DMSO). To assay the activity of the extracts, 10 μl dissolved extract in DMSO (or 10 μl DMSO as negative control) was put onto the bacterial lawn of a 3 cm Petri dish. After 1 hr, two L4 worms were put onto the plate, and the progeny were scored for Daf-c or Mig phenotypes after 3 days.

Rescue of the *daf-36* Phenotypes by Steroids

(25S),26-3-keto-4-cholestenoic acid (Δ^4-dafachronic acid), 4-cholesten-3-one, lathosterone, and lathosterol were obtained from the Mangelsdorf lab (Motola et al., 2006). Cholesterol and 7-dehydrocholesterol were obtained from Sigma-Aldrich. Compounds were diluted in 100% ethanol. Tests were performed on 3 cm NG agar plates seeded with a mixture of 90 μl 5× concentrated overnight culture of OP50 and 10 μl compound (or ethanol as negative control). Final concentrations were calculated as equally distributed over the total volume of agar (3 ml). After 1 hr, about 150 synchronized eggs (obtained from gravid adults over a time span of 4 hr) were placed onto the dried lawn of bacteria. Strains tested were grown reproductively onto regular NG agar for two generations at 20ºC. Dauer formation was scored after 2 days at 27ºC.

Supplemental Data

Supplemental Data including the *daf-36* phylogenetic tree, multiple sequence alignment, and steroid rescue are available at http://www.developmentalcell.com/cgi/content/full/10/4/473/DC1/.

Acknowledgments

The authors would like to thank J.H. Thomas for the *nrc-1* and *ncr-2* strains, the CGC for other nematode strains, Y. Kohara for cDNAs, the Sanger Center for cosmid clones, and A. Fire for GFP vectors. We would also like to thank S. Pletcher and members of the Antebi lab for critical reading of the manuscript, and R. Niwa and H. Kataoka for communicating unpublished results. This work was supported by Baylor College of Medicine Seed Fund (A.A.), NIH (A.A., D.J.M.), NIH/NURSA (A.A., D.J.M.), European Union (A.A.), Max Planck Gesellschaft (A.A., B.G., V.R.), Glenn/AFAR BIG Award (A.A.), the Howard Hughes Medical Institute (D.J.M., C.L.C.), and the Robert A. Welch Foundation (D.J.M.).

Received: December 6, 2005
Revised: January 30, 2006
Accepted: February 2, 2006
Published online: March 22, 2006

References

Ailion, M., and Thomas, J.H. (2003). Isolation and characterization of high-temperature-induced dauer formation mutants in *Caenorhabditis elegans*. Genetics *165*, 127–144.

Antebi, A., Yeh, W.H., Tait, D., Hedgecock, E.M., and Riddle, D.L. (2000). *daf-12* encodes a nuclear receptor that regulates the dauer diapause and developmental age in *C. elegans*. Genes Dev *14*, 1512–1527.

Apfeld, J., and Kenyon, C. (1998). Cell nonautonomy of *C. elegans daf-2* function in the regulation of diapause and life span. Cell *95*, 199–210.

Arantes-Oliveira, N., Apfeld, J., Dillin, A., and Kenyon, C. (2002). Regulation of life-span by germ-line stem cells in *Caenorhabditis elegans*. Science *295*, 502–505.

Bargmann, C.I., and Horvitz, H.R. (1991). Control of larval development by chemosensory neurons in *Caenorhabditis elegans*. Science *251*, 1243–1246.

Birnby, D.A., Link, E.M., Vowels, J.J., Tian, H., Colacurcio, P.L., and Thomas, J.H. (2000). A transmembrane guanylyl cyclase (DAF-11) and Hsp90 (DAF-21) regulate a common set of chemosensory behaviors in *C. elegans*. Genetics *155*, 85–104.

Chitwood, D.J. (1999). Biochemistry and function of nematode steroids. Crit. Rev. Biochem. Mol. Biol. *34*, 273–284.

Coburn, C.M., Mori, I., Ohshima, Y., and Bargmann, C.I. (1998). A cyclic nucleotide-gated channel inhibits sensory axon outgrowth in larval and adult *C. elegans*: a distinct pathway for maintenance of sensory axon structure. Development *125*, 249–258.

Feng, J., Bussiere, F., and Hekimi, S. (2001). Mitochondrial electron transport is a key determinant of life span in *Caenorhabditis elegans*. Dev. Cell *1*, 633–644.

Gerisch, B., and Antebi, A. (2004). Hormonal signals produced by DAF-9/cytochrome P450 regulate *C. elegans* dauer diapause in response to environmental cues. Development *131*, 1765–1766.

Gerisch, B., Weitzel, C., Kober-Eisermann, C., Rottiers, V., and Antebi, A. (2001). A hormonal signaling pathway influencing *C. elegans* metabolism, reproductive development, and life span. Dev. Cell *1*, 841–851.

Gill, M.S., Held, J.M., Fisher, A.L., Gibson, B.W., and Lithgow, G.J. (2004). Lipophilic regulator of a developmental switch in *Caenorhabditis elegans*. Aging Cell *3*, 413–421.

Gray, J., Wardzala, E., Yang, M., Reinbothe, S., Haller, S., and Pauli, F. (2004). A small family of LLS1-related non-heme oxygenases in plants with an origin amongst oxygenic photosynthesizers. Plant Mol. Biol. *54*, 39–54.

Hsin, H., and Kenyon, C. (1999). Signals from the reproductive system regulate the lifespan of *C. elegans*. Nature *399*, 362–366.

Inoue, T., and Thomas, J.H. (2000). Targets of TGF-beta signaling in *C. elegans* dauer formation. Dev Biology *217*, 192–204.

Ioannou, Y.A. (2001). Multidrug permeases and subcellular cholesterol transport. Nat. Rev. Mol. Cell Biol. *2*, 657–668.

Iwata, S., Saynovits, M., Link, T.A., and Michel, H. (1996). Structure of a water soluble fragment of the 'Rieske' iron-sulfur protein of the bovine heart mitochondrial cytochrome bc1 complex determined by MAD phasing at 1.5 Å resolution. Structure *4*, 567–579.

Jia, K., Albert, P.S., and Riddle, D.L. (2002). DAF-9, a cytochrome P450 regulating *C. elegans* larval development and adult longevity. Development *129*, 221–231.

Jiang, H., Parales, R.E., Lynch, N.A., and Gibson, D.T. (1996). Site-directed mutagenesis of conserved amino acids in the alpha subunit of toluene dioxygenase: potential mononuclear non-heme iron coordination sites. J. Bacteriol. *178*, 3133–3139.

Komatsu, H., Mori, I., Rhee, J.S., Akaike, N., and Ohshima, Y. (1996). Mutations in a cyclic nucleotide-gated channel lead to abnormal thermosensation and chemosensation in *C. elegans*. Neuron *17*, 707–718.

Li, W., Kennedy, S.G., and Ruvkun, G. (2003). *daf-28* encodes a *C. elegans* insulin superfamily member that is regulated by environmental cues and acts in the DAF-2 signaling pathway. Genes Dev. *17*, 844–858.

Li, J., Brown, G., Ailion, M., Lee, S., and Thomas, J.H. (2004). NCR-1 and NCR-2, the *C. elegans* homologs of the human Niemann-Pick type C1 disease protein, function upstream of DAF-9 in the dauer formation pathways. Development *131*, 5741–5752.

Libina, N., Berman, J.R., and Kenyon, C. (2003). Tissue-specific activities of *C. elegans* DAF-16 in the regulation of lifespan. Cell *115*, 489–502.

Mak, H.Y., and Ruvkun, G. (2004). Intercellular signaling of reproductive development by the *C. elegans* DAF-9 cytochrome P450. Development *131*, 1777–1786.

Matyash, V., Entchev, E.V., Mende, F., Wilsch-Brauninger, M., Thiele, C., Schmidt, A.W., Knolker, H.J., Ward, S., and Kurzchalia, T.V. (2004). Sterol-derived hormone(s) controls entry into diapause in *Caenorhabditis elegans* by consecutive activation of DAF-12 and DAF-16. PLoS Biol. *2*, e280.

Motola, D.L., Cummins, C.L., Rottiers, V., Sharma, K., Li, T., Sunino, K., Xu, E., Auchus, R., Antebi, A., and Mangelsdorf, D.J. (2006). Identification of hormonal ligands for the orphan nuclear receptor DAF-12 that govern Dauer formation and reproduction in *C. elegans*. Cell *124*, 1–15.

Murakami, M., Koga, M., and Ohshima, Y. (2001). DAF-7/TGF-β expression required for the normal larval development in *C. elegans* is controlled by a presumed guanylyl cyclase DAF-11. Mech. Dev. *109*, 27–35.

Murphy, C.T., McCarroll, S.A., Bargmann, C.I., Fraser, A., Kamath, R.S., Ahringer, J., Li, H., and Kenyon, C. (2003). Genes that act downstream of DAF-16 to influence the lifespan of *Caenorhabditis elegans*. Nature *424*, 277–283.

Ohkura, K., Suzuki, N., Ishihara, T., and Katsura, I. (2003). SDF-9, a protein tyrosine phosphatase-like molecule, regulates the L3/dauer developmental decision through hormonal signaling in *C. elegans*. Development *130*, 3237–3248.

Que, L., Jr. (2000). One motif–many different reactions. Nat. Struct. Biol. *7*, 182–184.

Riddle, D.L., and Albert, P.S. (1997). Genetic and Environmental Regulation of Dauer Larva Development. In *C. elegans* II, D.L. Riddle, B. Meyer, J. Priess, and T. Blumenthal, eds. (Cold Spring Harbor, NY, Cold Spring Harbor Laboratory Press).

Schackwitz, W.S., Inoue, T., and Thomas, J.H. (1996). Chemosensory neurons function in parallel to mediate a pheromone response in *C. elegans*. Neuron *17*, 719–728.

Schmidt, C.L., and Shaw, L. (2001). A comprehensive phylogenetic analysis of Rieske and Rieske-type iron-sulfur proteins. J. Bioenerg. Biomembr. *33*, 9–26.

Sulston, J., and Hodgkin, J. (1988). Methods. In The Nematode, *Caenorhabditis elegans*, W.B. Wood, ed. (Cold Spring Harbor, NY: Cold Spring Harbor Laboratory Press), pp. 587–606.

Sym, M., Basson, M., and Johnson, C. (2000). A model for niemann-pick type C disease in the nematode *C. elegans*. Curr. Biol. *10*, 527–530.

Sze, J.Y., Victor, M., Loer, C., Shi, Y., and Ruvkun, G. (2000). Food and metabolic signalling defects in a *C. elegans* serotonin-synthesis mutant. Nature *403*, 560–564.

Tissenbaum, H.A., Hawdon, J., Perregaux, M., Hotez, P., Guarente, L., and Ruvkun, G. (2000). A common muscarinic pathway for diapause recovery in the distantly related nematode species *Caenorhabditis elegans* and *Ancylostoma caninum*. Proc. Natl. Acad. Sci. USA *97*, 460–465.

van der Geize, R., Hessels, G.I., van Gerwen, R., van der Meijden, P., and Dijkhuizen, L. (2002). Molecular and functional characterization of *kshA* and *kshB*, encoding two components of 3-ketosteroid 9α-hydroxylase, a class IA monooxygenase, in *Rhodococcus erythropolis* strain SQ1. Mol. Microbiol. *45*, 1007–1018.

White, J.G., Southgate, E., Thomson, J.N., and Brenner, S. (1976). The structure of the ventral nerve cord of *Caenorhabditis elegans*. Philos. Trans. R. Soc. Lond. B Biol. Sci. *275*, 327–348.

Wicks, S.R., Yeh, R.T., Gish, W.R., Waterston, R.H., and Plasterk, R.H. (2001). Rapid gene mapping in *Caenorhabditis elegans* using a high density polymorphism map. Nat. Genet. *28*, 160–164.

Yochem, J., Gu, T., and Han, M. (1998). A new marker for mosaic analysis in *C. elegans* indicates a fusion between hyp6 and hyp7, two major components of the hypodermis. Genetics *149*, 1323–1334.

Supplemental Data

Hormonal Control of *C. elegans* Dauer Formation and Life Span by a Rieske-like Oxygenase

Veerle Rottiers, Daniel L. Motola, Birgit Gerisch, Carolyn L. Cummins, Kiyoji Nishiwaki, David J. Mangelsdorf, and Adam Antebi

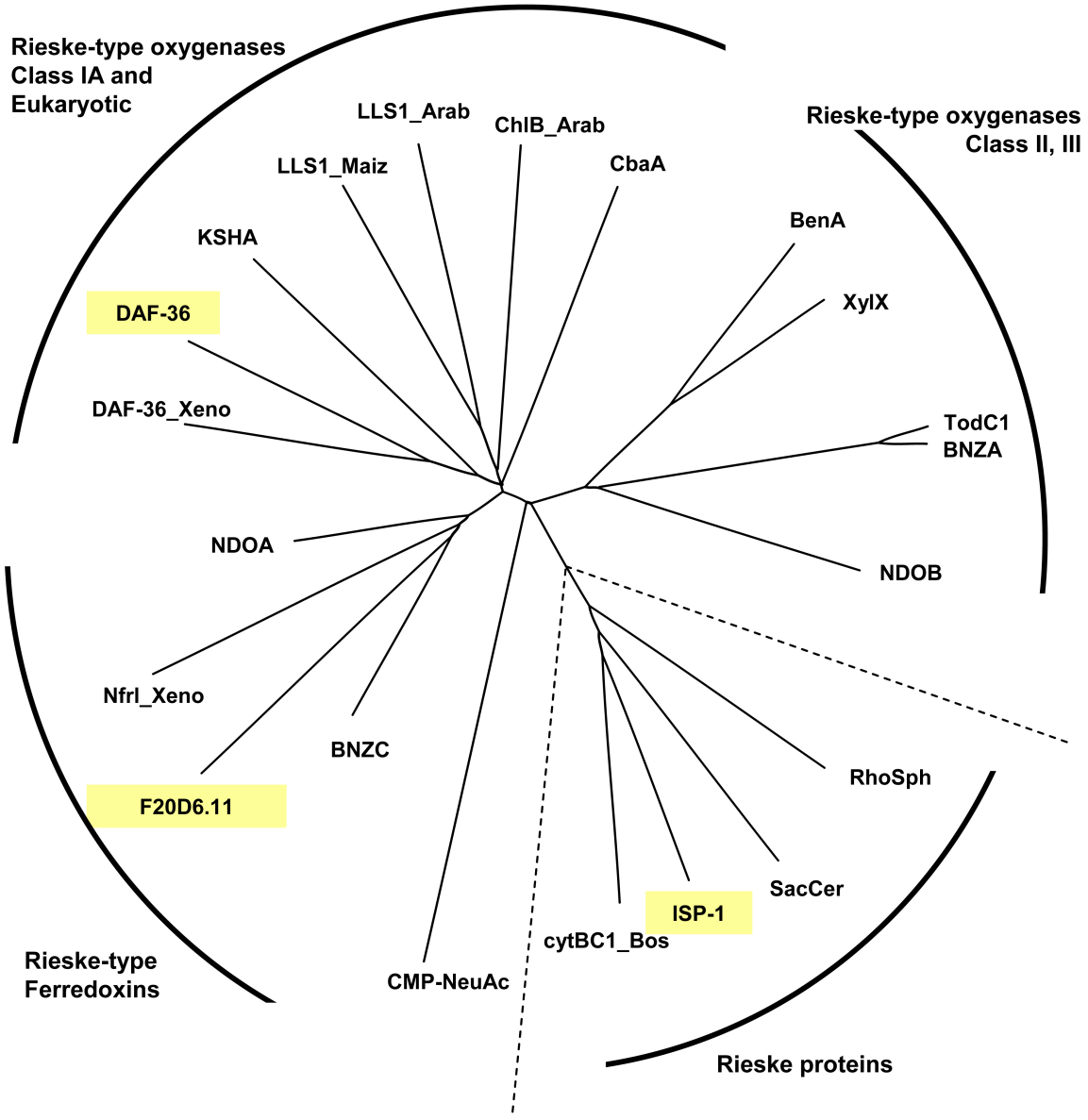

Figure S1. Phylogenetic tree showing the *C. elegans* proteins with a Rieske iron sulfur domain (DAF-36, ISP-1 and F20D6.11, in yellow boxes) in relation to other Rieske iron sulfur proteins. Rieske-type oxygenases: *DAF-36*_Xeno, based on cDNAs BJ625632, AW872227 and BJ616540 of *Xenopus laevis*; *KSHA*, 3-ketosteroid-9α-hydroxylase from *Rhodococcus erythropolis* (AAL96829) (van der Geize et al., 2002); LLS1_Maiz, lethal leaf spot 1 from Zea Mays (U77436))(Gray et al., 1997); LLS1_Arab, lethal leaf spot 1 of *Arabidopsis thaliana* (U77347)(Gray et al., 1997); ChlB_Arab, chlorophyll a oxygenase of *Arabidopsis thaliana* (T52458)(Tomitani et al., 1999); CbaA, 3-chlorobenzoate-3,4-dioxygenase from *Alcaligenes sp* (Q44256)(Nakatsu et al., 1995); BenA,

benzoate-1,2-dioxygenase from *Acintetobacter sp* (AF009224)(Neidle et al., 1991); XylX, benzoate-1,2-dioxygenase from *Pseudomonas putida* (M64747)(Harayama et al., 1991); TodC1, toluene dioxygense from *Pseudomonas putida* (J04996.1(Zylstra et al., 1989); BNZA, benzene 1,2-dioxygenase from *Pseudomonas putida* (P08084)(Irie et al., 1987); NDOB, naphthalene dioxygenase from *Pseudomonas putida* (M23914)(Kurkela et al., 1988); CMP-NeuAc is CMP-Neu5Ac hydroxylase from *Mus musculus* (A56469)(Kawano et al., 1994); Rieske proteins: SacCer, RIP1 of *Saccharomyces cerevisae* (P08067)(Beckmann et al., 1987); CytBC1_Bos, Cytochrome Bc1 complex protein of *Bos thaurus* (P13272)(Brandt et al., 1993); RhoSph, protein of *Rhodopseudomonas sphaeroides* (CAA27194)(Davidson and Daldal, 1987); Rieske-type ferredoxins: BZNC, benzene-1,2-dioxygenase from *Pseudomonas putida* (P08086)(Irie et al., 1987); NDOA, naphthalene dioxygenase from *Pseudomonas putida* (JN0643)(Kurkela et al., 1988); Nfrl_Xeno, ferredoxin of *Xenopus laevis* (BAA22375)(Hatada et al., 1997).

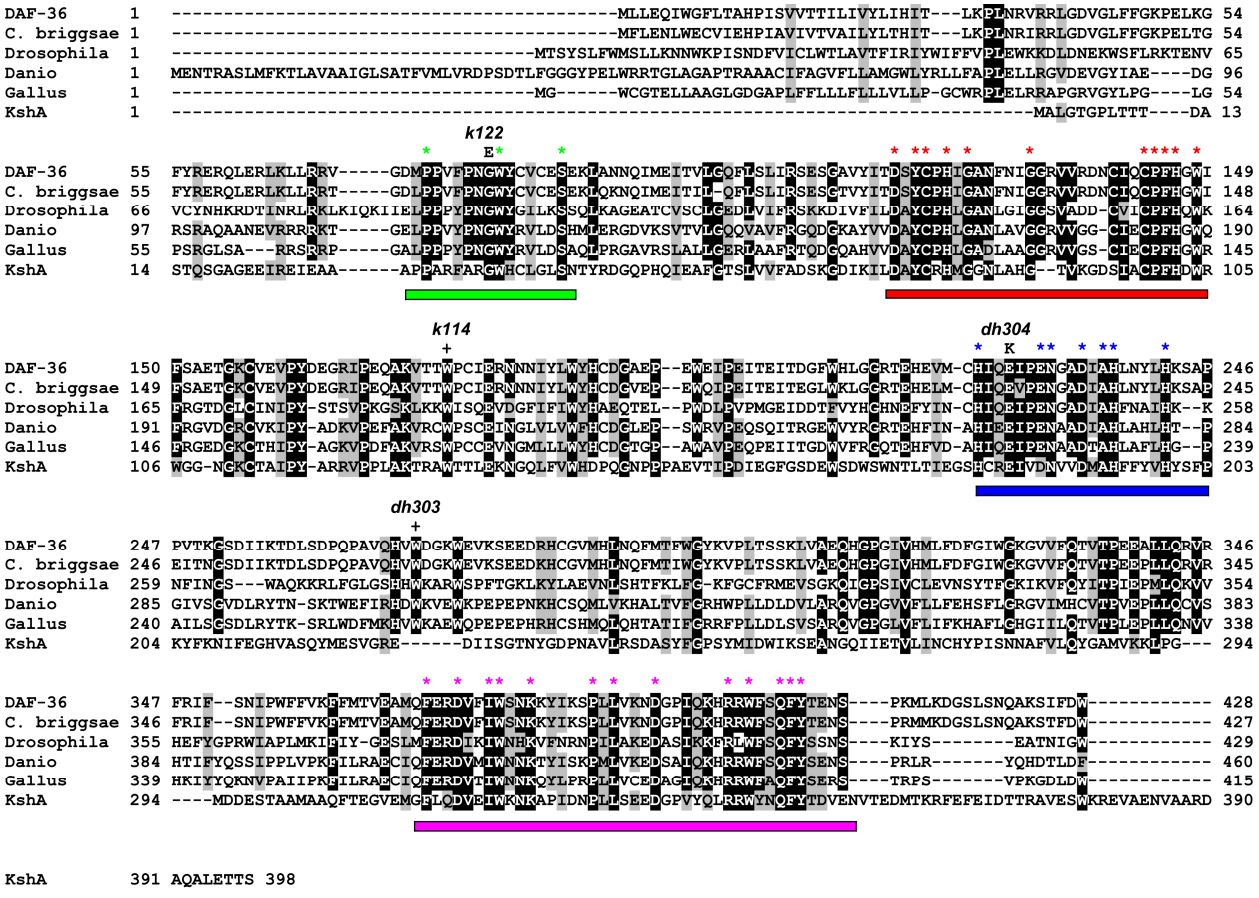

Figure S2. Multiple sequence alignment of DAF-36 with its closest homologs. Positions at which 80% identity is found are marked black, AA with same properties are marked in grey. The Rieske iron sulfur domain is marked in red, the non-heme iron domain is marked in blue, N-terminal domain is marked in green, C-terminal domain in pink. Conserved amino acids for domains are marked with *. Amino acid changes of mutations are shown on top. +, stop codons. DAF-36 is C12D8.5 wormbase protein CE34156, *C. briggsae* is *Caenorhabditis briggsae* protein CBG095563, *Drosophila* is *Drosophila melanogaster* protein CG40050 (NP_10153), *Danio* is *Danio rerio* predicted protein zgc:92275, *Gallus* is *Gallus gallus* predicted protein XP_425346.1, *kshA* is *Rhodococcus erythropolis* protein AAL96829 (van der Geize et al., 2002).

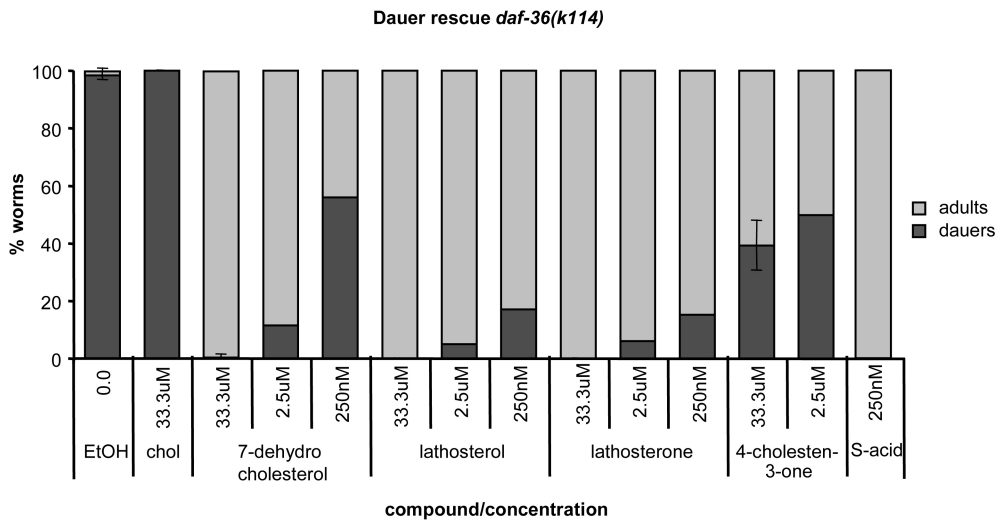

Figure S3. Rescue of dauer formation of *daf-36(k114)* at 27°C by steroid compounds. Chol is cholesterol, S-acid is Δ^4-dafachronic acid. Error bars are shown for the 33.3 μM concentration and represent the standard deviation derived from at least two independent experiments.

Supplemental Experimental Procedures for Figure S1:

Analysis was based on Schmidt and Shaw (Schmidt and Shaw, 2001). The sequences of the Rieske and Rieske type proteins used in the analysis were retrieved from GenBank via PubMed (accession numbers in legend) (http://www.ncbi.nlm.nih.gov/PubMed/). Selection of proteins was based on representative members of groups defined by Schmidt and Shaw (Schmidt and Shaw, 2001), sequences of *C. elegans* Rieske genes (as found in Wormbase release WS115) and DAF-36 homologs were added. Since proteins largely differ in homology and length, 200aa of each protein was selected starting 50aa before the first C of the Rieske iron binding domain (and thus including the non-heme iron binding domain, if present). Multiple sequence alignment of these sequences was done with ClustalW using T-Coffee software (http://www.ch.embnet.org/software/TCoffee.html)(Notredame et al., 2000). The phylogenetic tree was drawn by Phylodendron version 0.8d beta (http://iubio.bio.indiana.edu/treeapp/treeprint-form.html) based on the T-Coffee dendrogram file.

Supplemental References

Beckmann, J. D., Ljungdahl, P. O., Lopez, J. L., and Trumpower, B. L. (1987). Isolation and characterization of the nuclear gene encoding the Rieske iron-sulfur protein (RIP1) from Saccharomyces cerevisiae. J Biol Chem *262*, 8901-8909.

Brandt, U., Yu, L., Yu, C. A., and Trumpower, B. L. (1993). The mitochondrial targeting presequence of the Rieske iron-sulfur protein is processed in a single step after insertion into the cytochrome bc1 complex in mammals and retained as a subunit in the complex. J Biol Chem *268*, 8387-8390.

Davidson, E., and Daldal, F. (1987). fbc operon, encoding the Rieske Fe-S protein cytochrome b, and cytochrome c1 apoproteins previously described from Rhodopseudomonas sphaeroides, is from Rhodopseudomonas capsulata. J Mol Biol *195*, 25-29.

Gray, J., Close, P. S., Briggs, S. P., and Johal, G. S. (1997). A novel suppressor of cell death in plants encoded by the Lls1 gene of maize. Cell *89*, 25-31.

Harayama, S., Rekik, M., Bairoch, A., Neidle, E. L., and Ornston, L. N. (1991). Potential DNA slippage structures acquired during evolutionary divergence of Acinetobacter calcoaceticus chromosomal benABC and Pseudomonas putida TOL pWW0 plasmid xylXYZ, genes encoding benzoate dioxygenases. J Bacteriol *173*, 7540-7548.

Hatada, S., Kinoshita, M., Sakumoto, H., Nishihara, R., Noda, M., and Asashima, M. (1997). A novel gene encoding a ferredoxin reductase-like protein expressed in the neuroectoderm in Xenopus neurula. Gene *194*, 297-299.

Irie, S., Doi, S., Yorifuji, T., Takagi, M., and Yano, K. (1987). Nucleotide sequencing and characterization of the genes encoding benzene oxidation enzymes of Pseudomonas putida. J Bacteriol *169*, 5174-5179.

Kawano, T., Kozutsumi, Y., Kawasaki, T., and Suzuki, A. (1994). Biosynthesis of N-glycolylneuraminic acid-containing glycoconjugates. Purification and characterization of the key enzyme of the cytidine monophospho-N-acetylneuraminic acid hydroxylation system. J Biol Chem *269*, 9024-9029.

Kurkela, S., Lehvaslaiho, H., Palva, E. T., and Teeri, T. H. (1988). Cloning, nucleotide sequence and characterization of genes encoding naphthalene dioxygenase of Pseudomonas putida strain NCIB9816. Gene *73*, 355-362.

Nakatsu, C. H., Straus, N. A., and Wyndham, R. C. (1995). The nucleotide sequence of the Tn5271 3-chlorobenzoate 3,4-dioxygenase genes (cbaAB) unites the class IA oxygenases in a single lineage. Microbiology *141 (Pt 2)*, 485-495.

Neidle, E. L., Hartnett, C., Ornston, L. N., Bairoch, A., Rekik, M., and Harayama, S. (1991). Nucleotide sequences of the Acinetobacter calcoaceticus benABC genes for benzoate 1,2-dioxygenase reveal evolutionary relationships among multicomponent oxygenases. J Bacteriol *173*, 5385-5395.

Notredame, C., Higgins, D. G., and Heringa, J. (2000). T-Coffee: A novel method for fast and accurate multiple sequence alignment. J Mol Biol *302*, 205-217.

Schmidt, C. L., and Shaw, L. (2001). A comprehensive phylogenetic analysis of Rieske and Rieske-type iron-sulfur proteins. J Bioenerg Biomembr *33*, 9-26.

Tomitani, A., Okada, K., Miyashita, H., Matthijs, H. C., Ohno, T., and Tanaka, A. (1999). Chlorophyll b and phycobilins in the common ancestor of cyanobacteria and chloroplasts. Nature *400*, 159-162.

van der Geize, R., Hessels, G. I., van Gerwen, R., van der Meijden, P., and Dijkhuizen, L. (2002). Molecular and functional characterization of kshA and kshB, encoding two components of 3-ketosteroid 9alpha-hydroxylase, a class IA monooxygenase, in Rhodococcus erythropolis strain SQ1. Mol Microbiol *45*, 1007-1018.

Zylstra, G. J., Wackett, L. P., and Gibson, D. T. (1989). Trichloroethylene degradation by Escherichia coli containing the cloned Pseudomonas putida F1 toluene dioxygenase genes. Appl Environ Microbiol *55*, 3162-3166.